Evaluating bathymetric LiDAR accuracy with different sources of reference data

Jan Rhomberg-Kauert[1], Lucas Dammert[1], Laure-Anne Gueguen[1], Tomasz Kogut[2], Florian Pöppl[1,3], Roland Schwarz[3], Martin Pfennigbauer[4], Małgorzata Jarząbek-Rychard[5] and Gottfried Mandlburger[1]

[1]Department of Geodesy and Geoinformation, TU Wien; 1040 Vienna, Austria
- jan.rhomberg-kauert@geo.tuwien.ac.at, lucas.dammert@geo.tuwien.ac.at,
laure-anne.gueguen@geo.tuwien.ac.at, gottfried.mandlburger@geo.tuwien.ac.at
[2] Maritime University of Szczecin, Poland - t.kogut@pm.szczecin.pl
[3]*RIEGL* Laser Measurement Systems GmbH; 3480 Horn, Austria - fpoeppl@riegl.com
[4]*RIEGL* Research and Defense GmbH; 3480 Horn, Austria - mpfennigbauer@riegl.com
[5] Institute of Geodesy and Geoinformatics, Wrocław University of Environmental and Life Sciences
- malgorzata.jarzabek-rychard@upwr.edu.pl

Keywords: bathymetric LiDAR , SONAR, total station measurements, single-beam echo sounder, multi-beam echo sounder, ranging bias

Abstract

In order to provide proof of consistent quality, survey systems, acquisition methods, and procedures for analyzing the resulting data are subject to regular validation. One method of validation is punctual comparison with data for comparison that entitles as reference data. However, as the conditions at the time of data acquisition critically impact each survey, dedicated parallel surveys employing different methods. This can provide insight into discrepancies and relative consistencies, especially for research purposes. In the literature, multiple techniques and sensors have been presented for the acquisition of underwater reference data, such as multi-beam echo sounders, single-beam echo sounders, and different types of pole measurements. Furthermore, bathymetric LiDAR can be deployed from UAVs, helicopters, and aircraft, each entailing specific data resolution and accuracy. Therefore, this study presents four different bathymetric LiDAR datasets (one UAV, two helicopter and one airplane-based), where for each dataset a different type of reference acquisition approach is used appropriate for the individual water bodies (river, ponds, coastal waters). The results of this comparison display the overall alignment of bathymetric LiDAR and reference data with the highest accuracies for UAV data and pole reference measurements. There, the mean normal distance between the LiDAR data and the reference is $0\,\mathrm{cm} \pm 2\,\mathrm{cm}$ standard deviation. The highest difference was seen for the Baltic sea dataset, where airplane-based data and single-beam echo sounder reference were used. In this dataset, the mean normal distance between the LiDAR data and reference is $-5\,\mathrm{cm} \pm 10\,\mathrm{cm}$ standard deviation. In conclusion, the analyzed bathymetric LiDAR datasets show strong consistency with their respective reference measurements, with observed variations primarily influenced by environmental conditions and system configurations.

1. Introduction

For remote sensing of bathymetric data, different evaluation methods have been proposed and tested to acquire *reference data* (Dammert et al., 2025b; Mandlburger et al., 2025; Menna et al., 2024). Although terminology differs for the dataset used to evaluate bathymetry data in the literature (Bakuła et al., 2019; Maas et al., 2019; Mader et al., 2019), the selected term *reference data* refers in this study to the independently acquired data used in the comparison of the bathymetric LiDAR data and does not necessarily mean higher accuracy data. In general, the type of reference data is related to the amount of work required to obtain a complete dataset (Dammert et al., 2025b; Rhomberg-Kauert et al., 2025).

LiDAR can provide high-resolution data, but to assess its accuracy, the data needs to be compared to an independent, secondary data source (Mandlburger, 2022; Pfennigbauer et al., 2025). Although scanners are calibrated in laboratory environments prior to deployment (Pfennigbauer and Ullrich, 2010), especially airborne LiDAR often requires additional post-processing such as strip adjustment and alignment of multi-temporal data to achieve the highest accuracies (Dammert et al., 2025b; Mandlburger et al., 2025).

Evaluation of LiDAR data becomes considerably more difficult in submerged environments, as more challenging factors such as modeling the water surface, refraction correction, turbidity, and sensor positioning come into play (Mandlburger, 2022; Mandlburger et al., 2025; Schwarz et al., 2019). Different studies have compared LiDAR to data from single-beam echo sounders (SBES) or multi-beam echo sounders (MBES) (Costa et al., 2009; Do et al., 2020; Kinzel et al., 2013), and used pole-based total station measurements as comparative data for shallow waters (Dammert et al., 2025b; Mandlburger et al., 2025). However, underwater reference data present the unique challenge that in deeper or turbid water the measured reference data cannot be seen.

To evaluate bathymetric LiDAR, this study presents four bathymetric LiDAR datasets of different environments and different types of reference data. The study sites include coastal and inland waters (Section 2) with LiDAR survey platforms ranging from UAV, helicopter, and airplanes (Section 2). The reference data consists of two types of total station measurements, SBES and MBES data (Section 2). For each study site, the difference between the LiDAR point cloud and the reference is evaluated using three different metrics (Section 3), (i) the absolute vertical distance, (ii) normal plane distance, and (iii) relative vertical distance between LiDAR and reference data. The results are then presented and discussed in Section 4, which presents the observed consistencies and discrepancies between bathymetric

https://doi.org/10.5194/isprs-archives-XLVIII-1-W6-2025-191-2025 |

Dataset	Sensor	Platform	Range [m]	Scan frequency [kHz]	Beam divergence [mrad]	Reference data
A	*RIEGL* VQ-840-GL	UAV	60	200	1.0	Prism pole + Total station
B	*RIEGL* VQ-840-GL	Helicopter	160	100	3.0	Dual-prism pole + Total station
C	*RIEGL* VQ-840-G	Helicopter	100	100	3.0	Multi-beam echo sounder
D	*RIEGL* VQ-880-G II	Airplane	550	200	1.3	Single-beam echo sounder

Table 1. Parameters for the airborne laser scanning data acquisitions.

LiDAR and comparative data in real-world environments. For the purposes of a methodological comparison, we neglect the confidence levels of accuracy of the respective reference data. For an actual accuracy assessment, for example to determine conformity with specific quality criteria or with threshold values specified in published standards, the authority of the reference data would also have to be verified and suitably validated.

2. Materials

The deployed LiDAR systems and selected settings are shown in Table 1, for each study site, and a cross section of each study site is shown in Figure 1. The reference data for each dataset differ in terms of acquisition method. Two main types of reference data were acquired, SONAR data and pole measurements. The pole measurements (A and B) were acquired using a two-person team with a total station and a prism mounted on a pole. For the SONAR data, SBES and MBES were used during two different field measurements (C and D).

LiDAR datasets A-C were processed using the Surface-Volume-Bottom (SVB) algorithm Schwarz et al. (2019). For dataset B, the SVB algorithm was used in combination with waveform stacking (i.e. a combination of spatially adjacent waveforms), which improves the signal-to-noise ratio. This enabled the detection of consistent bottom returns in more turbid waters and thus allowed to map the entirety of the Pielach Ponds. The LiDAR data of dataset D was processed using online waveform processing (OWP) (Pfennigbauer et al., 2014). After the initial echo extraction, each dataset was georeferenced and refraction correction was performed.

References for datasets A, B and C were acquired using total station measurements in combination with long-time GNSS measurements. The LiDAR point clouds were precisely geo-referenced using saddle-roof shaped reference planes (Mandlburger et al., 2023). Dataset D only uses GNSS

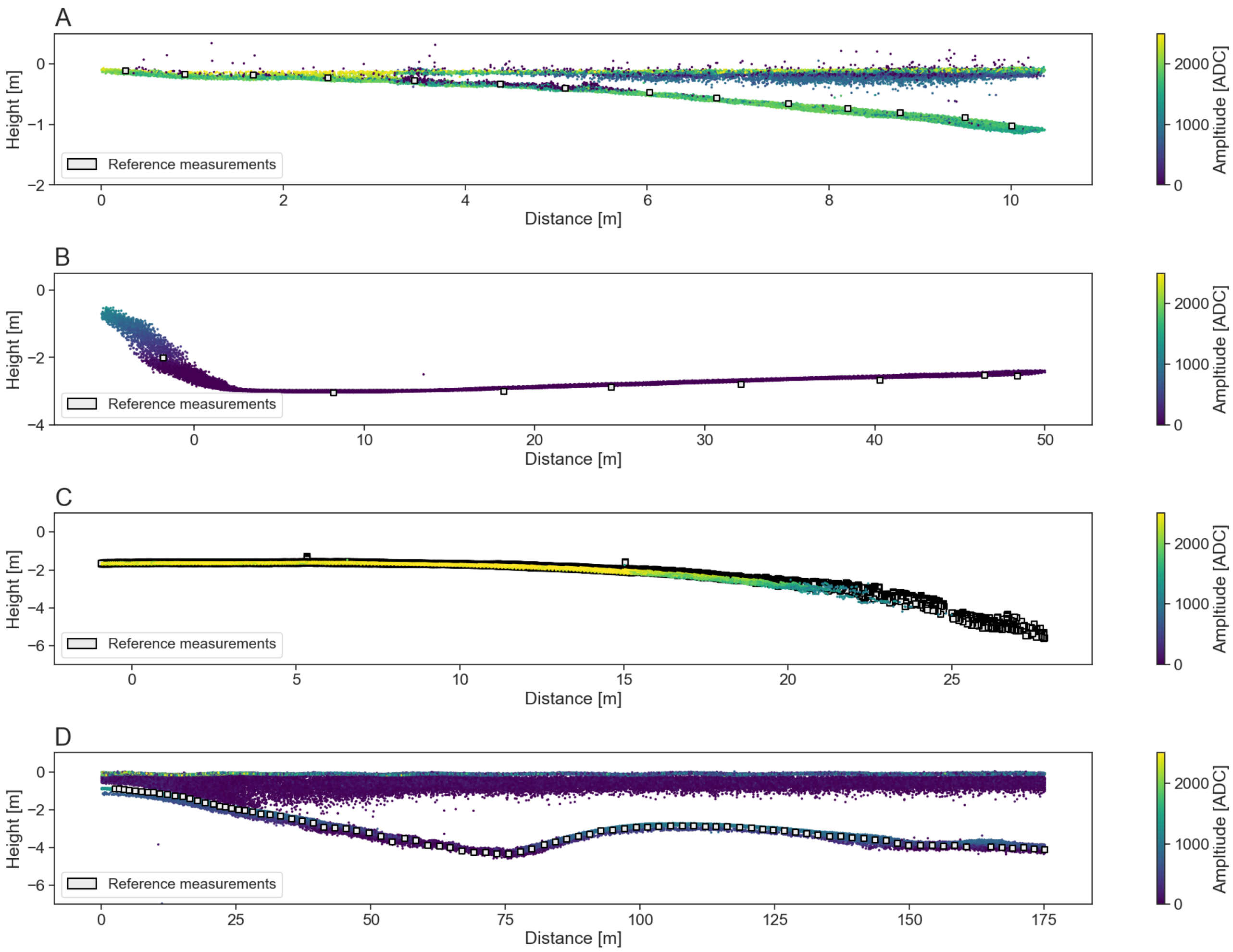

Figure 1. Cross section plot of datasets A-D together with the measured reference points. (A) Pielach River, (B) Pielach ponds, (C) Lake Erlauf and (D) Baltic Sea.

positioning for the survey vessel, which due to its lower measurement accuracy compared to total station measurements must be considered in the later accuracy evaluation. Regarding the reference measurement methods, the first dataset uses standard pole measurements with a $1.8\,\mathrm{m}$ measurement pole carried out by survey personnel in waders measuring each point with a total station. Dataset B builds on the newly developed method by Dammert et al. (2025b), which uses two total stations to simultaneously measure two prisms on top of a longer measurement pole and thus enables measurements for tilted, non-stationary poles. This was used to acquire reference data using a rowing boat and a measurement pole with a length of $4.5\,\mathrm{m}$. For dataset C, a small research vessel equipped with an MBES was used to acquire reference data. The trajectory of the vessel was acquired by a robotic total station, tracking a 360° prism mounted on the vessel (Dammert et al., 2025a). Based on the highly accurate trajectory (Dammert et al., 2025c) and the holistic georeferencing approach of Dammert et al. (2025a); Pöppl et al. (2024) an MBES dataset was computed, which provides high resolution reference data for the bathymetric LiDAR dataset. The reference data for dataset D was acquired using a research vessel for open water surveys, equipped with an SBES and georeferenced using GNSS-RTK.

3. Method

To align each reference dataset with the corresponding point cloud, two approaches were used. For datasets A, B and C, reference planes were set up and measured using a total station, these reference planes were identified within the LiDAR point cloud, and aligned to the planes measured by the total station. Each plane was measured with at least eight points from which a best-fitting plane was estimated. From these planes, a a synthetic point cloud was sampled, which were used to align the LiDAR point cloud using the iterative closest point algorithm. For dataset D, this was not possible. Therefore, the reference data and the LiDAR point cloud were aligned based on the GNSS-based trajectories.

To evaluate the discrepancies between the reference data and the LiDAR point cloud, three metrics were selected. These are (i) the absolute vertical distance to the nearest neighbor of the reference, (ii) the absolute plane distance to the reference, and (iii) the singed distance to the nearest neighbor of the reference (relative distance). These metrics are presented in detail in Equations 1, 2, and 4. Let for each reference point $p_i = (x_{p_i}, y_{p_i}, z_{p_i})$ be $n_i = (x_{n_i}, y_{n_i}, z_{n_i})$ the nearest neighbor of p_i. Then the absolute and relative vertical distances can be calculated by

$$\text{Abs. vertical distance :} \quad |d(p_i, n_i)| = |z_{p_i} - z_{n_i}| \quad (1)$$

$$\text{Rel. vertical distance :} \quad d(p_i, n_i) = z_{p_i} - z_{n_i}. \quad (2)$$

Furthermore, the normal vector of each LiDAR point n_i is given by $\vec{N}_i = (A_{n_i}, B_{n_i}, C_{n_i})$ (calculated by robust plane fitting using 32 nearest neighbors). With this, all plane parameters of n_i can be determined through

$$D = A_{n_i} \cdot x_{n_i} + B_{n_i} \cdot y_{n_i} - |C_{n_i}| \cdot z_{n_i}. \quad (3)$$

This can then be used to calculate the normal plane distance between p_i and n_i,

$$\text{Normal plane distance :} \frac{\big|Ax + By - |C|z - D\big|}{\sqrt{A^2 + B^2 + C^2}}. \quad (4)$$

For normal plane distances, normal vectors were calculated using the scientific point cloud processing software OPALS (Pfeifer et al., 2014) with a robust plane-fitting approach of the 32 nearest neighbors in the LiDAR point cloud. Furthermore, to evaluate the results of the metrics in comparison with the water depth of each reference, the water depth was calculated under the assumption of a planar water surface with the water height measured with the total station.

4. Results

The differences between the reference data and the bathymetric LiDAR data are compared in two steps. First, the differences are evaluated on a histogram basis. Secondly, these differences are shown in relation to the depth of the water. The aim of the first step is a general evaluation of reference and LiDAR data, while the secondary step aims to analyze potential biases for bathymetric LiDAR. Although we use the term *reference data* in all cases for the independently acquired data used to compare the LiDAR data, it must be noted that SBES and MBES data exhibit measurement uncertainties similar to LiDAR and that pole-based total station measurements also suffer from uncertainties concerning precise definition of the underwater points (gravel nuggets, mud, etc.). Thus, for the interpretation of the following results, it must be considered that both the uncertainty of the LiDAR as well as of the reference data impact the differences.

4.1 Accuracy estimation

The different scanner systems, platforms, and types of reference data display varying degrees of discrepancies (Figure 2). The main differences between the accuracies of the four datasets can be seen in the platform used to deploy the laser scanner (Figure 2 A - D). The UAV dataset mapped shallow and clear river waters and reference data was collected with a standard pole measurement. These ideal measurement conditions resulted in the overall low discrepancy.

For the two helicopter-based dataset (Figure 2 B and C) the distances to the reference points are mostly within $\pm 10\,\mathrm{cm}$ and the LiDAR data displays similar level of difference for both the MBES and dual-prism pole reference data, although the dual-prism pole displays a higher percentage of differences in the range of $\pm 10\,\mathrm{cm}$ to $20\,\mathrm{cm}$. The similarities between the two datasets reflect the similarity of the measurement characteristics for both bodies of water, as the Pielach ponds and Lake Erlauf are inland waters without current or tidal movements. Furthermore, the ponds are clear enough to allow full depth penetration for the Pielach ponds and measurements up to a depth of $10\,\mathrm{m}$ for Lake Erlauf. The differences between both datasets can potentially be explained by the types of sediment, as Pielach ponds have muddier terrain, where Lake Erlauf consists mainly of gravel and smaller rocks. Thus, pole measurements at the Pielach ponds face the challenge of potentially submerging the pole in the sediment, leading to a worse definition of the ground. This in combination with movement of the pole or bending during measurement introduces additional uncertainties during the reference data acquisition and therefore could explain the differences between the distributions of both datasets.

The last dataset (D) was measured along the coast of the Baltic Sea. Here, the turbulent waters of the surface zones and waves on the day of the survey present less suitable surveying conditions, and the discrepancies displayed are higher than those

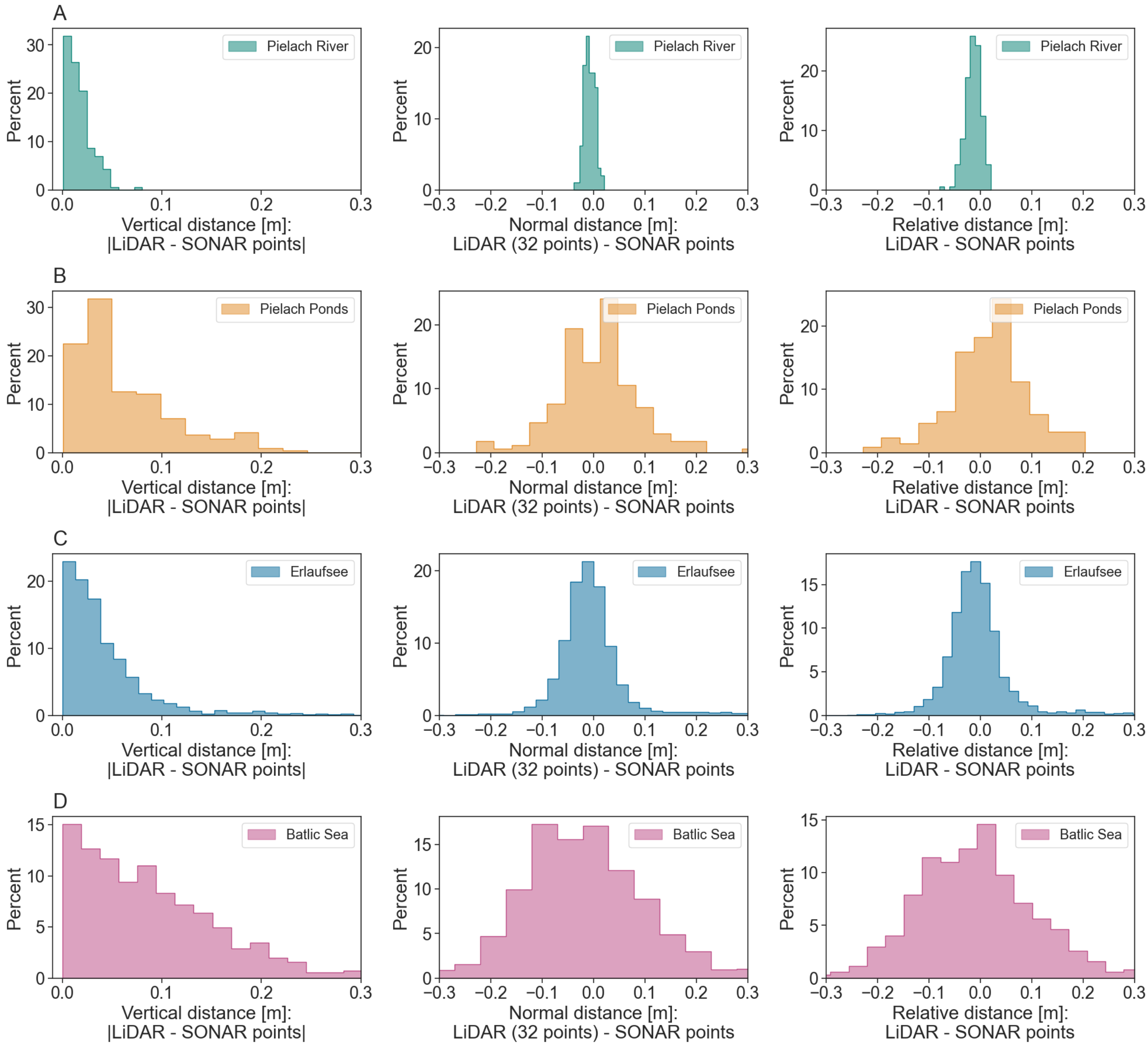

Figure 2. Histograms of the distance to reference for the absolute vertical distance, normal plane distance and relative vertical distance. (A) UAV dataset with standard pole measurement reference. (B) Helicopter dataset with dual-prism pole reference tracked with a total station. (C) Helicopter dataset with MBES reference dataset. (D) Airplane dataset with SBES reference.

of the previous dataset. Most of the data are contained within the range ±20 cm and the center is around zero. Furthermore, in contrast to previously considered reference measurements, the SBES used GNSS-RTK positions in contrast to total station measurements, which potentially lowers the accuracy of the reference data. Combined with the challenging refraction correction within the surf zone due to waves, the lower accuracy is expected for this data set.

4.2 Depth dependency

The UAV-based LiDAR point cloud and standard pole measurements display the lowest discrepancy, but are also limited to shallow waters of 1 m depth due to wader restriction (Figure 3). For helicopter-based surveys, the discrepancy is slightly higher with 1 σ mainly below ± 10 cm (Figure 3).

The newly introduced dual-prism pole method of Dammert et al. (2025b) displays discrepancies to the helicopter-based LiDAR data, similar to those observed for MBES, although 1 σ is not entirely within the 10 cm range. Both methods allow for mapping of deeper waters. Although the dual-prism pole can reach 4.65 m, MBES is capable of mapping the entirety of Lake Erlauf (maximum water depth of 38 m) exceeding the deepest LiDAR measurements, which are limited to about 10 m depth. The differences between the LiDAR and MBES data increase after a depth of 4 m. This is possibly related to lake topography, as Lake Erlauf is primary flat in the shallow zone and then slopes increase significantly toward the homogeneous bottom of the lake. Therefore, this change in mean deviation is possibly related to the angle of incidence rather than the depth of the water.

Lastly, the airplane-based dataset in the Baltic Sea displays the highest deviations, where the occurrence of waves, and the GNSS-based geo-referencing, pose more challenging measurement conditions and lower accuracy reference data. However, most of the data are still within the range of ± 10 cm (1 σ), with almost all data within ± 20 cm. Although the data do not dis-

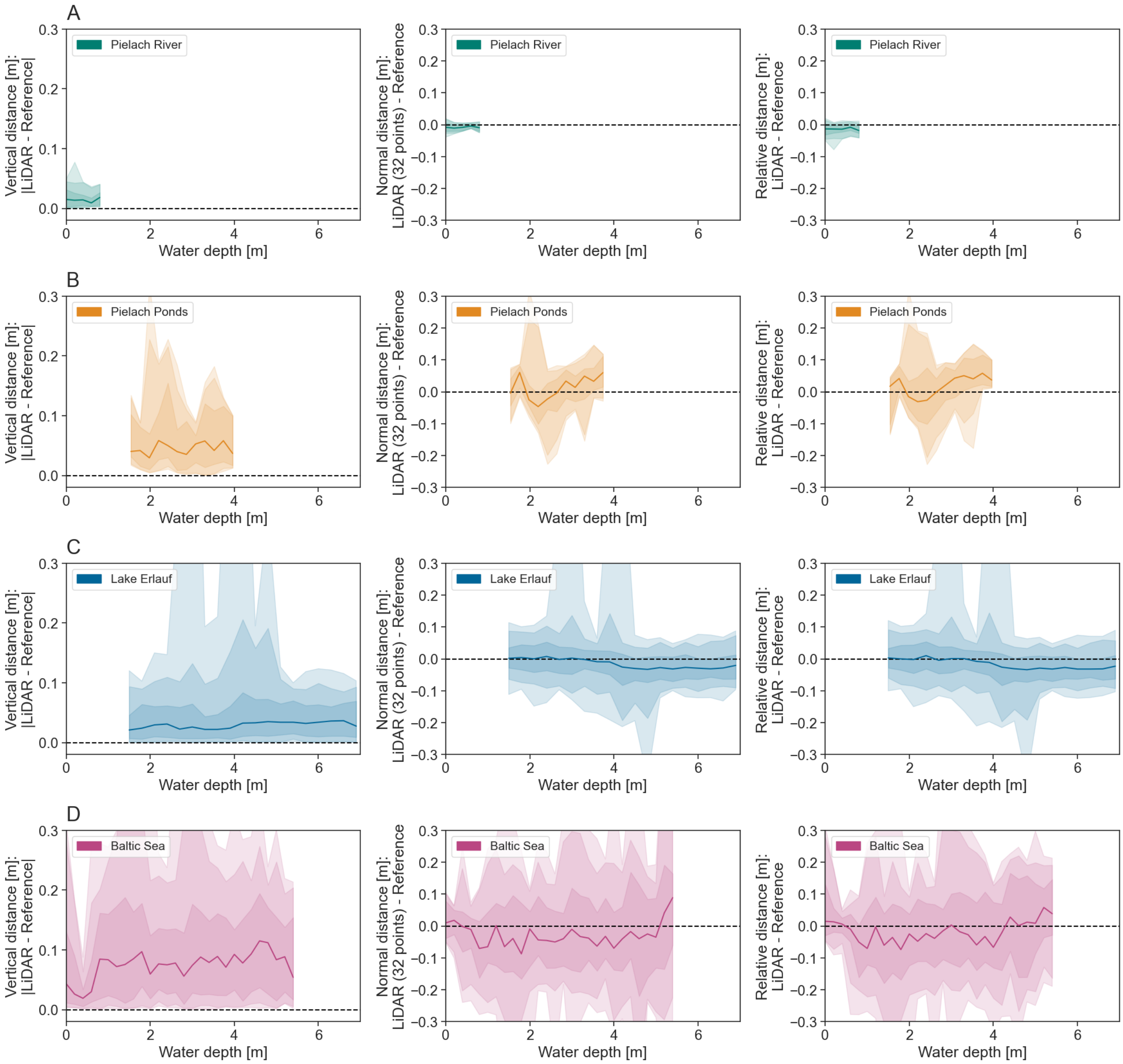

Figure 3. Distance to reference vs. water depth plot for the absolute vertical distance, normal plane distance and relative vertical distance. The different shadings correspond to 1, 2 and 3 σ (standard deviation), going from darker (1 σ) to lighter (3 σ). (A) UAV dataset with standard pole measurement reference. (B) Helicopter dataset with dual-prism pole reference. (C) Helicopter dataset with MBES reference dataset. (D) Airplane dataset with SBES reference.

play depth-dependent changes, the turbulent waters of the surf zone can be seen in the high fluctuation of the deviations from the reference data. In particular, the second and third standard deviations show a larger deviation of vertical differences between the LiDAR data and the reference data, compared to the other dataset.

5. Discussion

The differences between each reference and LiDAR dataset highlight the challenges of uncertainty evaluation for bathymetric LiDAR data. Factors such as platform, type of reference, and aquatic variables influence each evaluation. For the Pielach River, Pielach ponds and Lake Erlauf, the evaluation of accuracy based on the proposed methods, subject to their respective limitations and provided their validated quality, would result in compliance with the requirements of the IHO S-44 Special Order (IHO, 2008). However, while the IHO S-44 addresses the total vertical uncertainty (TVU) of a dataset, which can be estimated e.g. based on standard deviations of vertical depths (IHO, 2008), we focus on the vertical differences between two datasets. Thus, the differences obtained in our study can only indicate agreement of the data with the IHO S-44 standard and do not allow a final statement as the differences are always affected by the vertical uncertainty of both the LiDAR and the reference data. In the example of drone-based LiDAR and standard pole measurement comparison, the uncertainties estimated from these differences are lower than the TVU requirements of the IHO S-44 Exclusive Order (IHO, 2008).

For the dataset from the Baltic Sea (dataset D), the uncertainties estimated from the differences between LiDAR and SBES datasets slightly exceed the TVU requirements defined by IHO S-44 Special Order of $\sqrt{25\,\mathrm{cm}^2 + (0.0075 \cdot \mathrm{depth})^2}$ for some depths (Figure 3 D), although errors in the LiDAR dataset and the SBES reference dataset cannot be distinguished. For a real survey scenario requiring IHO conform deliverables, accuracy and consistency between the datasets could be improved for example by repeating the surveys under more favorable meteorological conditions. The slightly lower accuracy of airplane-based surveys has also been mentioned in other studies (Eren et al., 2019; Kastdalen et al., 2024), but providing examples of the conformity of airborne bathymetric LiDAR data with secondary data within a $25\,\mathrm{cm}$ TVU (Kastdalen et al., 2024) and highlighting challenges related to the influence of waves on LiDAR measurements (Birkebak et al., 2018; Eren et al., 2019). For the airplane-based measurements the larger measurement distance increases the effect of orientation uncertainties (roll, pitch and yaw). Furthermore, the larger footprint and higher speed, causes a lower point density, which can lead to worse results as point wise comparison might be not dense enough for ideal evaluation (Himmelsbach et al., 2025). Lastly, a larger footprint can cause problems when interacting with a highly inhomogeneous water surface, as, for example, waves can lead to a distortion of the footprint and thus lead to a lower accuracy (Birkebak et al., 2018; Eren et al., 2019).

Similarly, the high accuracy of UAV or helicopter-based surveys is well documented in the literature (Mano et al., 2020; Kastdalen et al., 2024; Wang et al., 2022). There, the increase in point density due to lower flying altitude and reduced speed has been shown to increase coverage and capture the underwater topography of the surveyed area with higher resolution and accuracy (Kastdalen et al., 2024; Himmelsbach et al., 2025). However, these studies also highlight the differences in accuracy depending on the water bodies surveyed and the challenges e.g., in fast moving waters (Awadallah et al., 2023; Kastdalen et al., 2024; Himmelsbach et al., 2025), as well as potential inaccuracies due to rough water surfaces (Birkebak et al., 2018). Therefore, the accuracy of bathymetric LiDAR is dependent not only on the type of reference data but also on the water body surveyed and the airborne system used.

In addition to the differences presented, factors such as angle of incidence must also be considered in the accuracy analysis as, especially for dataset B, the lake bottom slopes drastically after a depth of $4\,\mathrm{m}$, potentially causing the change in the data visible in Figure 3 C. Such errors have not been thoroughly explored at this point and could potentially affect the depth-dependent total vertical uncertainty estimations, seen in previous studies regarding bathymetric LiDAR accuracy (Pfennigbauer et al., 2025).

6. Conclusion

Our study presents four different datasets. In each dataset, bathymetric LiDAR deployed from different survey platforms were compared to different kinds of reference data. The reference data ranges from total station measurements to acoustic measurements. This comparison provides insights into the vertical uncertainty between the underwater datasets. Furthermore the different types of reference data outlines a fundamental question of what reference data can look like in bathymetric surveys, as well as highlighting the challenges in the evaluation of bathymetric datasets. For the dataset analyzed, UAV surveys under ideal river surveying conditions display the highest accuracy, with helicopter surveys also satisfying IHO S-44 Special Order requirements. However, the airplane-based dataset (dataset D) displays a lower consistency with the reference data, potentially caused by rough water surface and generally more difficult survey conditions. Furthermore, for the Lake Erlauf dataset, the shift of the median vertical difference between the bathymetric LiDAR and reference data with increased depth could correspond to the angle of incidence rather than the depth of the water, which needs to be further studied in future work. In general, the comparison highlights the difference between the different water bodies and systems used, emphasizing the high accuracy of bathymetric LiDAR under favorable surveying conditions.

7. Acknowledgments

The authors gratefully acknowledge VERBUND AG and BOKU University for their support in the MBES data acquisition at Lake Erlauf. Furthermore, the authors sincerely thank GisPro for providing the LiDAR and SBES datasets from the Baltic Sea used in this evaluation. Their support and data contributions were essential to conduct this research and ensure the robustness of the analysis.

References

Awadallah, M. O. M., Malmquist, C., Stickler, M., Alfredsen, K., 2023. Quantitative Evaluation of Bathymetric LiDAR Sensors and Acquisition Approaches in Lærdal River in Norway. *Remote Sensing*, 15(1), 263.

Bakuła, K., Mills, J. P., Remondino, F., 2019. A REVIEW OF BENCHMARKING IN PHOTOGRAMMETRY AND REMOTE SENSING. *The International Archives of the Photogrammetry, Remote Sensing and Spatial Information Sciences*, XLII-1/W2, 1–8.

Birkebak, M., Eren, F., Pe'eri, S., Weston, N., 2018. The Effect of Surface Waves on Airborne Lidar Bathymetry (ALB) Measurement Uncertainties. *Remote Sensing*, 10(3), 453.

Costa, B., Battista, T., Pittman, S., 2009. Comparative evaluation of airborne LiDAR and ship-based multibeam SoNAR bathymetry and intensity for mapping coral reef ecosystems. *Remote Sensing of Environment*, 113(5), 1082–1100.

Dammert, L., Pöppl, F., Rhomberg-Kauert, J., Thalmann, T., Monetti, D., Neuner, H.-B., Mandlburger, G., 2025a. Leveraging robotic total stations and multi-sensor adjustment for accurate multibeam bathymetry. *The International Hydrographic Review*, 31(2).

Dammert, L., Rhomberg-Kauert, J., Thalmann, T., Gueguen, L.-A., Monetti, D., Neuner, H.-B., Mandlburger, G., 2025b. Accurate reference for shallow water bathymetry using a tilt-compensating dual-prism pole and time-synchronized robotic total stations. *The International Archives of the Photogrammetry, Remote Sensing and Spatial Information Sciences*, XLVIII-2/W10-2025, 55–62.

Dammert, L., Thalmann, T., Pöppl, F., Monetti, D., Neuner, H.-B., Mandlburger, G., 2025c. High-precision geo-referencing of UAS data with robotic total stations. *ISPRS Annals of the Photogrammetry, Remote Sensing and Spatial Information Sciences*, 213–220.

Do, J. D., Jin, J.-Y., Kim, C. H., Kim, W.-H., Lee, B.-G., Wie, G. J., Chang, Y. S., 2020. Measurement of Nearshore Seabed Bathymetry Using Airborne/Mobile LiDAR and Multibeam Sonar at Hujeong Beach, Korea. *Journal of Coastal Research*, 95(sp1), 1067.

Eren, F., Jung, J., Parrish, C. E., Sarkozi-Forfinski, N., Calder, B. R., 2019. Total Vertical Uncertainty (TVU) Modeling for Topo-Bathymetric LIDAR Systems. *Photogrammetric Engineering amp; Remote Sensing*, 85(8), 585–596.

Himmelsbach, T., Rhomberg-Kauert, J., Mandlburger, G., Dobler, W., Gems, B., Aufleger, M., 2025. Airborne and UAV-borne Laser Bathymetry applied to a mountain river reach. *The International Archives of the Photogrammetry, Remote Sensing and Spatial Information Sciences*, XLVIII-2/W10-2025, 131–138.

IHO, 2008. S-44, Standards for Hydrographic Surveys. Standard 5th ed., International Hydrographic Organization, Monaco.

Kastdalen, L., Stickler, M., Malmquist, C., Heggenes, J., 2024. Evaluating methods for measuring in-river bathymetry: Remote sensing green LIDAR provides high-resolution channel bed topography limited by water penetration capability. *River Research and Applications*, 40(4), 467–482.

Kinzel, P. J., Legleiter, C. J., Nelson, J. M., 2013. Mapping river bathymetry with a small footprint green LiDAR: applications and challenges 1. *JAWRA Journal of the American Water Resources Association*, 49(1), 183–204.

Maas, H.-G., Mader, D., Richter, K., Westfeld, P., 2019. IMPROVEMENTS IN LIDAR BATHYMETRY DATA ANALYSIS. *The International Archives of the Photogrammetry, Remote Sensing and Spatial Information Sciences*, XLII-2/W10, 113–117.

Mader, D., Richter, K., Westfeld, P., Weiß, R., Maas, H.-G., 2019. DETECTION AND EXTRACTION OF WATER BOTTOM TOPOGRAPHY FROM LASERBATHYMETRY DATA BY USING FULL-WAVEFORM-STACKING TECHNIQUES. *The International Archives of the Photogrammetry, Remote Sensing and Spatial Information Sciences*, XLII-2/W13, 1053–1059.

Mandlburger, G., 2022. A review of active and passive optical methods in hydrography. *The International Hydrographic Review*, 8–52.

Mandlburger, G., Kölle, M., Pöppl, F., Cramer, M., 2023. EVALUATION OF CONSUMER-GRADE AND SURVEY-GRADE UAV-LIDAR. *The International Archives of the Photogrammetry, Remote Sensing and Spatial Information Sciences*, XLVIII-1/W3-2023, 99–106.

Mandlburger, G., Rhomberg-Kauert, J., Gueguen, L.-A., Mulsow, C., Brezovsky, M., Dammert, L., Haines, J., Glas, S., Himmelsbach, T., Schulte, F. et al., 2025. Mapping shallow inland running waters with UAV-borne photo and laser bathymetry: The Pielach River showcase. *Hydrographische Nachrichten*, 130(03), 42–53.

Mano, K., Sakai, K., Tachibana, K., Sakita, K., Nishiyama, S., 2020. THE MEASUREMENT ACCURACY AND MEASUREMENT CHARACTERISTICS OF GREEN LiDAR DRONE. *The International Archives of the Photogrammetry, Remote Sensing and Spatial Information Sciences*, XLIII-B1-2020, 479–483.

Menna, F., Nocerino, E., Calantropio, A., 2024. High-accuracy height differences using a pressure sensor for ground control points measurement in underwater photogrammetry. *The International Archives of the Photogrammetry, Remote Sensing and Spatial Information Sciences*, XLVIII-2-2024, 273-279. Copernicus, https://doi.org/10.5194/isprs-archives-XLVIII-2-2024-273-2024.

Pfeifer, N., Mandlburger, G., Otepka, J., Karel, W., 2014. OPALS–A framework for Airborne Laser Scanning data analysis. *Computers, Environment and Urban Systems*, 45, 125–136.

Pfennigbauer, M., Haring, A., Riegl, U., Spitzer, A., 2025. TPU Estimation for Bathymetric LiDAR. *The International Archives of the Photogrammetry, Remote Sensing and Spatial Information Sciences*, 48, 215–221.

Pfennigbauer, M., Ullrich, A., 2010. Improving quality of laser scanning data acquisition through calibrated amplitude and pulse deviation measurement. *Laser Radar Technology and Applications XV*, 7684, SPIE, 463–472.

Pfennigbauer, M., Wolf, C., Weinkopf, J., Ullrich, A., 2014. Online waveform processing for demanding target situations. M. D. Turner, G. W. Kamerman, L. M. Wasiczko Thomas, E. J. Spillar (eds), *Laser Radar Technology and Applications XIX; and Atmospheric Propagation XI*, 9080, SPIE, 90800J.

Pöppl, F., Ullrich, A., Mandlburger, G., Pfeifer, N., 2024. A flexible trajectory estimation methodology for kinematic laser scanning. *ISPRS Journal of Photogrammetry and Remote Sensing*, 215, 62–79.

Rhomberg-Kauert, J., Himmelsbach, T., Pöppl, F., Dammert, L., Pfennigbauer, M., Mandlburger, G., 2025. Mapping river topography in whitewater rapids using bathymetric LiDAR.

Schwarz, R., Mandlburger, G., Pfennigbauer, M., Pfeifer, N., 2019. Design and evaluation of a full-wave surface and bottom-detection algorithm for LiDAR bathymetry of very shallow waters. *ISPRS journal of photogrammetry and remote sensing*, 150, 1–10.

Wang, D., Xing, S., He, Y., Yu, J., Xu, Q., Li, P., 2022. Evaluation of a New Lightweight UAV-Borne Topo-Bathymetric LiDAR for Shallow Water Bathymetry and Object Detection. *Sensors*, 22(4), 1379.